Simulation of Plasmonics Nanodevices with Coupled Maxwell and Schrödinger Equations using the FDTD Method

Iftikhar Ahmed and Erping Li

Department of Electronics and Photonics
A*STAR, Institute of High Performance Computing, Singapore
*corresponding author, E-mail: iahmed@ihpc.a-star.edu.sg

Abstract

A numerical approach that couples Lorentz-Drude model incorporated Maxwell equations with Schrödinger equation is presented for the simulation of plasmonics nanodevices. Maxwell equations with Lorentz-Drude (LD) dispersive model are applied to large size components, whereas coupled Maxwell and Schrödinger equations are applied to components where quantum effects are needed. The finite difference time domain method (FDTD) is applied to simulate these coupled equations. Numerical results of the coupled approach are compared with the conventional approach.

1. Introduction

The miniaturization of devices and high speed data are main challenges with existing silicon based technologies, and the reasons behind are diffraction limit and RC time delay respectively. For the solution of such challenges different efforts have been done in the past, however, an area known as plasmonics has been introduced recently to handle them, and it has shown promising applications [1-3]. Plasmonics deals with collective oscillation of free electrons at the interface of dielectric and metal, which remain bounded to the surface. Plasmonics is generally categorized into surface plasmon polaritons (SPP) and localized surface plasmon resonance (LSPR). The first one is more suitable for information transmission related applications, while the second one is preferable for sensing applications. A wide range of plasmonic devices have been simulated, fabricated and characterized [1-10]. Some interesting results show that the surface plasmon polariton has strong analogy to Young's double–slit experiment and is discussed in [4]. The concept of semiconductor plasmonics using a solid state model that includes Pauli exculsion principle, state filling effect, Fermi-Dirac thermalization, and external magnetic field is presented in [5]. A numerical approach that consists of solid state and Lorentz-Drude models is presented to simulate active plasmonics devices [6]; and it is also used to simulate a plasmonic source, and then light extraction from the source [7]. Some other active plasmonic devices such as Plas-MOStor (plasmonic based transistor), ultrafast active devices, passive and active photonics circuits using SPP have been reported in [8-10]. The concept of replacing the conventional gold and silver with doped semiconductors and intermetallics has been discussed in [11].

Plasmonic based phenomena have potential to handle the challenges with existing CMOS and photonics technologies, and can be used to interface photonics and electronics devices effectively. However, modeling and simulation of such interfacing domains become complex due to different scales of components. These complexities can be solved by implying different techniques. Nonetheless, when the size of a device reduces to a few nanometers, quantum effects dominate and their considerations become important to maintain the accuracy. Therefore, to incorporate them into modeling and simulation techniques, modifications in the conventional numerical techniques are needed, whereas conventional numerical techniques have performed well for the simulation of bulk materials and devices.

For quantum effects there is need to adopt some appropriate approaches from quantum mechanics, and usually Schrödinger equation is considered to incorporate such effects. On the other hand Maxwell equations are used for electromagnetic effects. Therefore, these equations are coupled to simulate those applications in which combined effects are needed [12-13]. In [12] a hybrid transmission line matrix (TLM) [14] and FDTD [15], and in [13] a hybrid locally one dimensional (LOD)-FDTD [16] and FDTD methods are applied to coupled non-dispersive Maxwell and Schrödinger equations. In [12] the FDTD method is applied to Schrödinger equation to simulate carbon nanotube while the TLM method is applied to the conventional non-dispersive Maxwell equations to simulate the rest of the structure. Whereas in [13], the FDTD method is applied to Schrödinger equation to simulate a semiconductor nanowire and the LOD-FDTD method is applied to the conventional non-dispersive Maxwell equations to simulate rest of the structure efficiently. In brief, in [12-13] hybrid approaches are applied to nanotube, nanowire and non dispersive materials.

In this paper, as compared to the [12-13], the LD dispersive model [17] incorporated Maxwell equations are coupled with Schrödinger equation to simulate plasmonic nanodevices. Schrödinger equation incorporated Maxwell equations are applied to simulate the components in which quantum effects are needed. The FDTD method is applied to simulate these coupled equations. In section 2, detailed formulation of the Maxwell equations with LD model, formulation of the Schrödinger equation in the presence of external electromagnetic field, and discretization using the FDTD method are presented. The reason of using LD model as compared to the other dispersive models is because of its better accuracy for broader range of wavelength. In section 3, numerical results of the coupled approach are compared with those from the conventional Maxwell approach and at the end conclusion is given.

2. Formulations

The time dependent Maxwell equations with frequency dependent permittivity and quantum current density are written as

$$\mu \frac{\partial H}{\partial t} = -\nabla \times E \tag{1}$$

$$\varepsilon(\omega)\frac{\partial E}{\partial t} = \nabla \times H - J_q \tag{2}$$

where J_q is quantum current density, and is obtained from Schrödinger equation. $\varepsilon(\omega) = \varepsilon_0 \varepsilon_r(\omega)$ is the frequency dependent permittivity and is obtained from Lorentz-Drude dispersive model. In the model, Drude part deals with intraband effects and is generally used for free electrons, whereas, the Lorentz model deals with interband effects and generally deals with bounded electrons. The LD model is written as

$$\varepsilon_r(\omega) = \varepsilon_\infty + \frac{\omega_{pD}^2}{j^2\omega^2 + j\Gamma_D\omega} + \frac{\Delta\varepsilon_L \omega_{pL}^2}{j^2\omega^2 + j\omega\Gamma_L + \omega_L^2} \tag{3}$$

where ω_{pD} is plasma frequency and Γ_D is damping constant associated with Drude model (intraband effects), ω_{pL} is plasma frequency, Γ_L is damping constant, and ω_L is resonance frequency of the first pole of Lorentz model (interband effects). After putting equation (3) into equation (2) and by using the auxiliary differential equation (ADE) approach, and some mathematical simplifications we get following equations

$$\nabla \times H = \varepsilon_0 \varepsilon_\infty \frac{\partial E}{\partial t} + Q + \frac{\varepsilon_0 \partial P}{\partial t} + J_q \tag{4}$$

$$\frac{\partial Q}{\partial t} = \omega_{pD}^2 \varepsilon_0 E - Q\Gamma_D \tag{5}$$

$$\frac{\partial^2 P}{\partial t^2} + \Gamma_L \frac{\partial P}{\partial t} + \omega_L^2 P = \Delta\varepsilon_L \omega_{pL}^2 E \tag{6}$$

Where terms with subscript D and term Q denote Drude model and terms with subscript L and term P denote Lorentz model. During the simulation of a structure with the proposed approach four different scenarios can arise i) a section of the structure in which there is no need of dispersive model and quantum current density, ii) a region in which quantum current density is required but not dispersive model, iii) a section in which dispersive model is needed but not quantum current density, iv) a region where both effects are needed. Under all these scenarios equation (2) will be effected. In this section, as an example formulation for the scenario (iv) is presented, however, it can be modified based on the situation.

After some mathematical simplifications equation (4) can be written as

$$\frac{\partial E_x}{\partial t} = \frac{1}{\varepsilon_0\varepsilon_\infty}\left(\frac{\partial H_z}{\partial y} - \frac{\partial H_y}{\partial z}\right) - \frac{Q_x}{\varepsilon_0\varepsilon_\infty} - \frac{1}{\varepsilon_\infty}\frac{\partial P_x}{\partial t} - \frac{1}{\varepsilon_0\varepsilon_\infty} J_{qx} \tag{7}$$

$$\frac{\partial E_y}{\partial t} = \frac{1}{\varepsilon_0\varepsilon_\infty}\left(\frac{\partial H_x}{\partial z} - \frac{\partial H_z}{\partial x}\right) - \frac{Q_y}{\varepsilon_0\varepsilon_\infty} - \frac{1}{\varepsilon_\infty}\frac{\partial P_y}{\partial t} - \frac{1}{\varepsilon_0\varepsilon_\infty} J_{qy} \tag{8}$$

$$\frac{\partial E_z}{\partial t} = \frac{1}{\varepsilon_0\varepsilon_\infty}\left(\frac{\partial H_y}{\partial x} - \frac{\partial H_x}{\partial y}\right) - \frac{Q_z}{\varepsilon_0\varepsilon_\infty} - \frac{1}{\varepsilon_\infty}\frac{\partial P_z}{\partial t} - \frac{1}{\varepsilon_0\varepsilon_\infty} J_{qz} \tag{9}$$

$$\frac{\partial H_x}{\partial t} = \frac{1}{\mu}\left(\frac{\partial E_y}{\partial z} - \frac{\partial E_z}{\partial y}\right) \tag{10}$$

$$\frac{\partial H_y}{\partial t} = \frac{1}{\mu}\left(\frac{\partial E_z}{\partial x} - \frac{\partial E_x}{\partial z}\right) \tag{11}$$

$$\frac{\partial H_z}{\partial t} = \frac{1}{\mu}\left(\frac{\partial E_x}{\partial y} - \frac{\partial E_y}{\partial x}\right) \tag{12}$$

The discritized form of the equations (7) to (9) is given as

$$\begin{aligned}
E_x^{n+1}(i+\tfrac{1}{2},j,k) &= \frac{1}{\Omega_x} E_x^{n}(i+\tfrac{1}{2},j,k) \\
&+ \frac{\Delta t}{\Omega_x \varepsilon_0 \varepsilon_\infty}\left[\begin{array}{l} \dfrac{H_z^{n+\frac{1}{2}}(i+\frac{1}{2},j+\frac{1}{2},k) - H_z^{n+\frac{1}{2}}(i+\frac{1}{2},j-\frac{1}{2},k)}{\Delta y} \\ -\dfrac{H_y^{n+\frac{1}{2}}(i+\frac{1}{2},j,k+\frac{1}{2}) - H_y^{n+\frac{1}{2}}(i+\frac{1}{2},j,k-\frac{1}{2})}{\Delta z} \end{array}\right] \\
&- \frac{\Delta t}{2\Omega_x \varepsilon_0 \varepsilon_\infty}\left[\begin{array}{l} \alpha_x Q_x^n(i+\frac{1}{2},j,k) + \beta_x E_x^n(i+\frac{1}{2},j,k) \\ + Q_x^n(i+\frac{1}{2},j,k) \end{array}\right] \\
&- \frac{1}{\Omega_x \varepsilon_\infty}\left[\begin{array}{l} \varsigma_x E_x^{n}(i+\frac{1}{2},j,k) + \tau_x P_x^n(i+\frac{1}{2},j,k) \\ -\rho_x P_x^{n-1}(i+\frac{1}{2},j,k) - P_x^n(i+\frac{1}{2},j,k) \end{array}\right] - \frac{1}{\varepsilon_0\varepsilon_\infty} J_{qx}^{n+1}(r)
\end{aligned} \tag{13}$$

$$
\begin{aligned}
E_y^{n+1}(i,j+\tfrac{1}{2},k) &= \frac{1}{\Omega_y} E_y^{\,n}(i,j+\tfrac{1}{2},k) \\
&+ \frac{\Delta t}{\Omega_y \varepsilon_0 \varepsilon_\infty}\left[\begin{array}{l} \dfrac{H_x^{n+\frac{1}{2}}(i,j+\frac{1}{2},k+\frac{1}{2}) - H_x^{n+\frac{1}{2}}(i,j+\frac{1}{2},k-\frac{1}{2})}{\Delta z} \\ -\dfrac{H_z^{n+\frac{1}{2}}(i+\frac{1}{2},j+\frac{1}{2},k) - H_z^{n+\frac{1}{2}}(i-\frac{1}{2},j+\frac{1}{2},k)}{\Delta x} \end{array}\right] \\
&- \frac{\Delta t}{2\Omega_y \varepsilon_0 \varepsilon_\infty}\left[\begin{array}{l} \alpha_y Q_y^n(i,j+\frac{1}{2},k) + \beta_y E_y^n(i,j+\frac{1}{2},k) \\ + Q_y^n(i,j+\frac{1}{2},k) \end{array}\right] \\
&- \frac{1}{\Omega_y \varepsilon_\infty}\left[\begin{array}{l} \varsigma_y E_y^{\,n}(i,j+\frac{1}{2},k) + \tau_y P_y^n(i,j+\frac{1}{2},k) \\ -\rho_y P_y^{n-1}(i,j+\frac{1}{2},k) - P_y^n(i,j+\frac{1}{2},k) \end{array}\right] - \frac{1}{\varepsilon_0 \varepsilon_\infty} J_{qy}^{n+1}(r)
\end{aligned} \tag{14}
$$

$$
\begin{aligned}
E_z^{\,n+1}(i,j,k+\tfrac{1}{2}) &= \frac{1}{\Omega_z} E_z^{\,n}(i,j,k+\tfrac{1}{2}) \\
&+ \frac{\Delta t}{\Omega_z \varepsilon_0 \varepsilon_\infty}\left[\begin{array}{l} \dfrac{H_y^{n+\frac{1}{2}}(i+\frac{1}{2},j,k+\frac{1}{2}) - H_y^{n+\frac{1}{2}}(i-\frac{1}{2},j,k+\frac{1}{2})}{\Delta x} \\ -\dfrac{H_x^{n+\frac{1}{2}}(i,j+\frac{1}{2},k+\frac{1}{2}) - H_x^{n+\frac{1}{2}}(i,j-\frac{1}{2},k+\frac{1}{2})}{\Delta y} \end{array}\right] \\
&- \frac{\Delta t}{2\Omega_z \varepsilon_0 \varepsilon_\infty}\left[\begin{array}{l} \alpha_z Q_z^n(i,j,k+\frac{1}{2}) + \beta_z E_z^{\,n}(i,j,k+\frac{1}{2}) \\ + Q_z^n(i,j,k+\frac{1}{2}) \end{array}\right] \\
&- \frac{1}{\Omega_z \varepsilon_\infty}\left[\begin{array}{l} \varsigma_z E_z^{\,n}(i,j,k+\frac{1}{2}) + \tau_z P_z^n(i,j,k+\frac{1}{2}) \\ -\rho_z P_z^{n-1}(i,j,k+\frac{1}{2}) - P_z^n(i,j,k+\frac{1}{2}) \end{array}\right] - \frac{1}{\varepsilon_0 \varepsilon_\infty} J_{qz}^{n+1}(r)
\end{aligned} \tag{15}
$$

Equations (5) and (6) are discritzed as

$$Q_r^{n+1} = \alpha_r Q_r^n + \beta_r \left[E_r^{n+1} + E_r^n\right] \tag{16}$$

$$P_r^{n+1} = \varsigma_r \left(E_r^{n+1} + E_r^n\right) + \tau_r P_r^n - \rho_r P_r^{n-1} \tag{17}$$

where

$$\alpha_r = \frac{\left(1 - \frac{\Delta t \Gamma_D}{2}\right)}{\left(1 + \frac{\Delta t \Gamma_D}{2}\right)}, \quad \beta_r = \frac{\frac{\Delta t \omega_{pD}^2 \varepsilon_0}{2}}{\left(1 + \frac{\Delta t \Gamma_D}{2}\right)}, \quad \Omega_r = \left(\frac{\varsigma_r}{\varepsilon_\infty} + 1 + \frac{\Delta t \beta_r}{2\varepsilon_0 \varepsilon_\infty}\right)$$

$$\varsigma_r = \frac{\frac{\Delta t^2 \Delta \varepsilon_L \omega_{pL}^2}{2}}{\left(1 + \Delta t \Gamma_L + \frac{\Delta t^2}{2}\omega_L^2\right)}, \quad \tau_r = \frac{\left(2 + \Delta t \Gamma_L - \frac{\Delta t^2}{2}\omega_L^2\right)}{\left(1 + \Delta t \Gamma_L + \frac{\Delta t^2}{2}\omega_L^2\right)},$$

$$\rho_r = \frac{1}{\left(1 + \Delta t \Gamma_L + \frac{\Delta t^2}{2}\omega_L^2\right)}$$

where $r = x$, y and z.

Equations (10) to (12) are similar to conventional magnetic field equations in FDTD method and are discritized as

$$
\begin{aligned}
H_x^{\,n+\frac{1}{2}}(i,j+\tfrac{1}{2},k+\tfrac{1}{2}) &= H_x^{\,n-\frac{1}{2}}(i,j+\tfrac{1}{2},k+\tfrac{1}{2}) \\
&+ \frac{\Delta t}{\mu}\left[\begin{array}{l} \dfrac{E_y^n(i,j+\frac{1}{2},k+1) - E_y^n(i,j+\frac{1}{2},k)}{\Delta z} \\ -\dfrac{E_z^n(i,j+1,k+\frac{1}{2}) - E_z^n(i,j,k+\frac{1}{2})}{\Delta y} \end{array}\right]
\end{aligned} \tag{18}
$$

$$
\begin{aligned}
H_y^{\,n+\frac{1}{2}}(i+\tfrac{1}{2},j,k+\tfrac{1}{2}) &= H_y^{\,n-\frac{1}{2}}(i+\tfrac{1}{2},j,k+\tfrac{1}{2}) \\
&+ \frac{\Delta t}{\mu}\left[\begin{array}{l} \dfrac{E_z^n(i+1,j,k+\frac{1}{2}) - E_z^n(i,j,k+\frac{1}{2})}{\Delta x} \\ -\dfrac{E_x^n(i+\frac{1}{2},j,k+1) - E_x^n(i+\frac{1}{2},j,k)}{\Delta z} \end{array}\right]
\end{aligned} \tag{19}
$$

$$
\begin{aligned}
H_z^{\,n+\frac{1}{2}}(i+\tfrac{1}{2},j+\tfrac{1}{2},k) &= H_z^{\,n-\frac{1}{2}}(i+\tfrac{1}{2},j+\tfrac{1}{2},k) + \\
&\frac{\Delta t}{\mu}\left[\begin{array}{l} \dfrac{E_x^n(i+\frac{1}{2},j+1,k) - E_x^n(i+\frac{1}{2},j,k)}{\Delta y} \\ -\dfrac{E_y^n(i+1,j+\frac{1}{2},k) - E_y^n(i,j+\frac{1}{2},k)}{\Delta x} \end{array}\right]
\end{aligned} \tag{20}
$$

Equations (13) to (20) represent discritized form of the Maxwell equations (equation 13 to 15 with LD model and quantum current density) after applying the FDTD method. For quantum effects the time dependent Schrödinger equation is considered in the presence of external electromagnetic field and is written as

$$i\hbar \frac{\partial \Psi(r,t)}{\partial t} = \left[\frac{1}{2m}\left[-i\hbar\nabla - qA(r,t)\right]^2 + q\Phi(r,t) + V(r)\right]\Psi(r,t) \tag{21}$$

where Ψ is wavefunction, A is vector potential, Φ is scalar potential, $\hbar = h/2\pi$, h is Planck constant, q is charge, m is mass of an electron and r represents spatial variables x, y, and z. The vector and scalar potentials are obtained from following equations

$$E = -\frac{\partial A}{\partial t} - \nabla.\Phi \quad , \quad H = \frac{1}{\mu}\nabla \times A$$

The equation (21) is complex, and by using the relation $\Psi(r,t) = \Psi_R(r,t) + i\Psi_I(r,t)$ and after some simplifications; it is separated into real and imaginary parts and is given as

$$
\begin{aligned}
\frac{\partial \Psi_R(r,t)}{\partial t} &= -\frac{\hbar}{2m}\frac{\partial^2 \Psi_I(r,t)}{\partial r^2} + \frac{q^2}{2\hbar m}\left(A(r,t)\right)^2 \Psi_I(r,t) \\
&- \frac{q}{2m}\frac{\partial A(r,t)}{\partial r}\Psi_R(r,t) - \frac{q}{m}A(r,t)\frac{\partial \Psi_R(r,t)}{\partial r} - \frac{q}{\hbar}\Phi(r,t)\Psi_I(r,t) \\
&+ \frac{1}{\hbar}V(r)\Psi_I(r,t)
\end{aligned} \tag{22}
$$

$$
\begin{aligned}
\frac{\partial \Psi_I(r,t)}{\partial t} &= \frac{\hbar}{2m}\frac{\partial^2 \Psi_R(r,t)}{\partial r^2} - \frac{q^2}{2\hbar m}\left(A(r,t)\right)^2 \Psi_R(r,t) \\
&- \frac{q}{2m}\frac{\partial A(r,t)}{\partial r}\Psi_I(r,t) - \frac{q}{m}A(r,t)\frac{\partial \Psi_I(r,t)}{\partial r} + \frac{q}{\hbar}\Phi(r,t)\Psi_R(r,t) \\
&- \frac{1}{\hbar}V(r)\Psi_R(r,t)
\end{aligned} \tag{23}
$$

Temporal discretization of equations (22) and (23) is given as

$$
\begin{aligned}
\Psi_R^{n+1}(r) &= \Psi_R^{n}(r) - \frac{\hbar\Delta t}{2m}\frac{\partial^2 \Psi_I^{n}(r)}{\partial r^2} + \frac{q^2\Delta t}{2\hbar m}\left(A^{n}(r)\right)^2 \Psi_I^{n}(r) \\
&- \frac{q\Delta t}{2m}\frac{\partial A^{n}(r)}{\partial r}\Psi_R^{n}(r) - \frac{q\Delta t}{m}A^{n}(r)\frac{\partial \Psi_R^{n}(r)}{\partial r} \\
&- \frac{q\Delta t}{\hbar}\Phi^{n}(r)\Psi_I^{n}(r) + \frac{\Delta t}{\hbar}V(r)\Psi_I^{n}(r)
\end{aligned} \tag{24}
$$

$$
\begin{aligned}
\Psi_I^{n+1}(r) &= \Psi_I^{n}(r) - \frac{\hbar\Delta t}{2m}\frac{\partial^2 \Psi_R^{n}(r)}{\partial r^2} + \frac{q^2\Delta t}{2\hbar m}\left(A^{n}(r)\right)^2 \Psi_R^{n}(r) \\
&- \frac{q\Delta t}{2m}\frac{\partial A^{n}(r)}{\partial r}\Psi_I^{n}(r) - \frac{q\Delta t}{m}A^{n}(r)\frac{\partial \Psi_I^{n}(r)}{\partial r} \\
&- \frac{q\Delta t}{\hbar}\Phi^{n}(r)\Psi_R^{n}(r) + \frac{\Delta t}{\hbar}V(r)\Psi_R^{n}(r)
\end{aligned} \tag{25}
$$

After calculating the real and imaginary parts of the wavefunction, and then by using the following relation, the quantum current density is obtained.

$$
J_q^{n+1}(r) = \frac{\hbar q}{2im}\left(\begin{aligned} &\Psi^{n+1^*}(r)\frac{\partial \Psi^{n+1}(r)}{\partial r} \\ &-\Psi^{n+1}(r)\frac{\partial \Psi^{n+1^*}(r)}{\partial r}\end{aligned}\right) - \frac{q^2}{m}\left|\Psi^{n+1}(r)\right|^2 A^{n+1}(r) \tag{26}
$$

Spatial discretization of equations (24-26) and the corresponding term $J_q^{n+1}(r)$ in equations (13-15) depends on the user how he/she want to implement these equations in one dimensional or three dimensional fashions. The meshing interface between Maxwell and Schrödinger equations also depends on one or three dimensional pattern of spatial discretization. We have used both patterns and found the similar results. For interface between Maxwell and Schrödinger equations, wave function, quantum current density and the corresponding electric field are discretized at same point. The value of quantum current density at interface or boundary of both domains is added up with electric field. In other words, the quantum current density can also be used as a source for the Maxwell equations i.e. at the boundary of Schrödinger equation, quantum current density is injected into Maxwell equations. The vector and scalar potentials are used to incorporate the external electromagnetic field into Schrödinger equation along the nanowire. In the simulation procedure, the magnetic field is updated first, then vector potential, scalar potential, wave function, quantum current density, and at the end electric field are updated and this sequence continues, until the last iteration.

3. Numerical Results

For numerical results two different examples that include dispersive and quantum effects are studied. A generalized structure is shown in Fig. 1, in which semiconductor nanowires are used as interconnects between plasmonics nanodevices. The size of plasmonics devices can be from few nanometer to few hundred nanometers, whereas the size of interconnects can be few nanometers. For such applications in the paper we use LD dispersive model for large size components, whereas Schrödinger equation is used for quantum effects needed region.

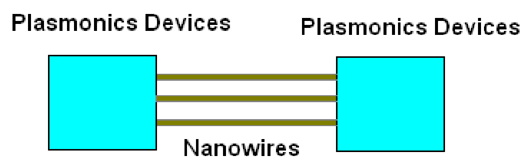

Fig. 1: A generalized structure for coupled approach, in which plasmonics devices are interconnected via nanowires.

The structures studied in the paper have operating concept similar to the generalized structure in Fig.1. The structure for the first example is shown in Fig. 2(a). It consists of two gold nanospheres, each with a radius of 20 nm, with a gap of 10 nm in between them, and a 2 nm thick and 70 nm long semiconductor nanowire (NW) is placed at center in between nanospheres. The purpose of the structure is to study the quantum effects and then comparison of the coupled and conventional approaches. The cell size in each direction is uniform i.e. 2nm. To maintain the stability of the Schrödinger equation with the FDTD method, the time step should be smaller than the Courant Friedrich Levy (CFL) limit of Maxwell equations [18]. Therefore, in the coupled approach, the time step of the Schrödinger equation is taken as the time step for whole simulation domain. We take time step 100 times smaller than that of the CLN limit to accommodate the NW, in other words, accuracy will also be better if the cell size is smaller. We have checked method with different grids or cell sizes and it is found that the proposed approach converges properly and in addition there is no stability issue, as long as the time step for the simulation domain is same as of Schrödinger equation. The parameters used for dispersive model are same as given in [17]. The surrounding medium of the structure is free space. A Gaussian pulse is used as a source to get field localization in between nanospheres and a Gaussian pulse at NW is used to excite the wavefunction. Four different field excitation scenarios may arise during the simulation of the structure, I) excitation that can generate field localization between nanospheres, II) source above or below the NW in the surrounding medium, III) use of quantum current density as a source, IV) combination of the above three scenarios. Figure 2 (b) shows snapshot of field localization in between nanospheres without having the NW in the *xy* plane, whereas Fig. 2 (c) depicts the snapshot of the total electric field intensity in the *xy* plane with nanowire. These both snapshots are obtained at steady state. In this application the excitation scenario (I) is used. Results show that most of the field is confined along the NW. Figure 2(d) shows the field intensity with and without Schrödinger equation with respect to number of time steps and depicts the difference between both circumstances. Figure 2 (e) is plotted with respect to energy (eV) with and without quantum effects. The difference of 0.16 eV is observed. The field observation point is at 26 nm away from the center of nanospheres and 12 nm left from the center of the NW. These results illustrate the clear difference between coupled and conventional approaches. The possible reason of the difference between the results of both approaches is quantum effect. Because in the case of coupled approach, the quantum current density takes into account, kinetic and potential energies of electrons, vector and scalar potentials. Inclusion of these factors is cause of shift in the field intensity in Fig. 2 (d and e). It is also observed that if the structure is made of bulk materials, then there is no difference in the numerical results of both approaches, and it is validation of the proposed approach.

The structure of second example is shown in Fig. 3 (a), in which two pairs of gold nanospheres are placed at both ends of the nanowire. The thickness and length of the NW, radius and distance between nanospheres is same as in example 1 at first, however, latter on the distance between nanospheres is varied.

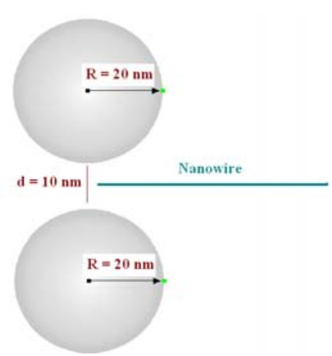

(a)

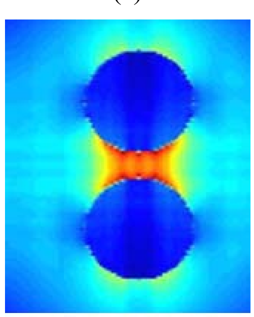

(b)

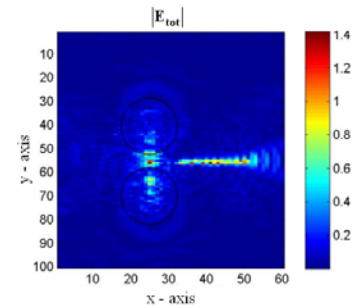

(c)

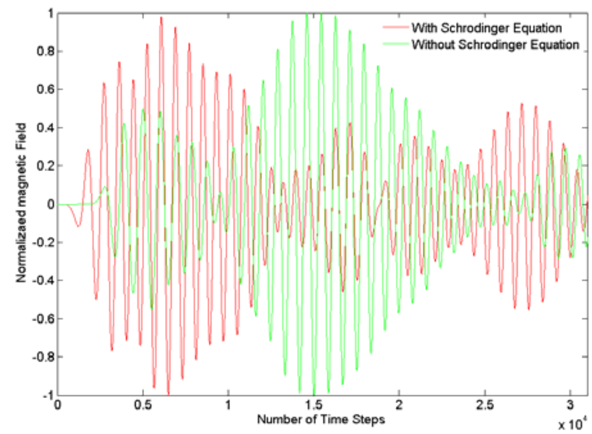

(d)

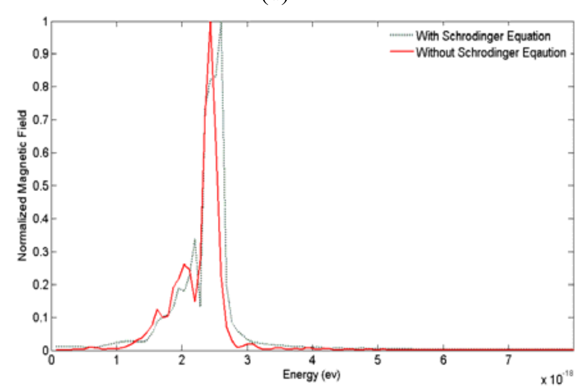

(e)

Fig. 2: (a) Structure for example 1, (b) Field intensity in the *xy* plane without nanowire (c) Field intensity in the *xy* plane with nanowire (d) Normalized magnetic field intensity with and without Schrödinger equation (e) Normalized field with respect to energy (eV).

Figure 3(b) shows the normalized electric field intensity near the center of the NW, under two different situations, i) the field is excited and localized between nanospheres at one-end of the NW (from example 1, green color line), ii) the field is excited and localized at both-ends of the NW (example 2, red color line). It represents that in the case of resonance field at one end (example 1), the field becomes weaker with the passage of time, while in the case of resonance field at both ends of the NW (example 2), amplitude of field remains stronger for longer time along the

NW. The reason of stronger field at NW in the second case is due to two sources i.e. at each end of the wire and this causes resonance for longer time.

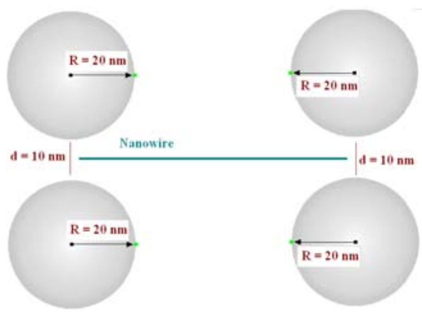

(a)

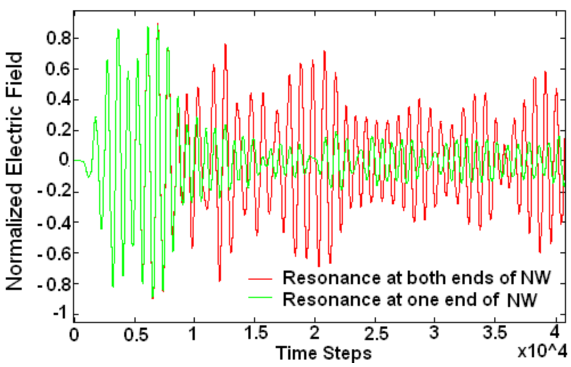

(b)

Fig. 3: (a) Structure for example 2, (b) Electric field at NW with localized field at one end and localized field at both ends of the nanowire.

These structures may have number of applications in different areas such as bio sensing, e.g. heating and blood sample analysis. Because of comparatively longer and stronger field oscillations, second example can be used for blood or liquid analysis more effectively as compared to the example 1. Figure 4 denotes the normalized field pattern for structure 3(a). In this case three different excitation sources are used, localized fields at both ends between nanospheres, and third close to the center of the NW. The field pattern in Fig. 4 (a) is captured during the transient state of the method, where a small value at the center of the NW shows the excitation of the wavefunction. Figures 4 (b) and 4 (c) show the electric and magnetic field patterns for same structure at steady state respectively. These field patterns describe that at steady state most of the field concentrates along the NW. However, the field values become weaker and weaker with the passage of time due to field radiation in the surrounding media. These patterns are captured when the gap distance between the nanospheres is 10 nm.
Nonetheless, the patterns and results are also studied for variable distance between nanospheres, and observed the similar phenomena but with different field intensities. Figure 5 shows the field plot of the structure with and without incorporating the Schrödinger equation. Figure 5 (a) indicates electric field intensity at NW with respect to number of time steps, dotted line shows the result without quantum effect and the solid line with quantum effects. Figure 5 (b) indicates the corresponding values of the electric field with respect to energy (eV).

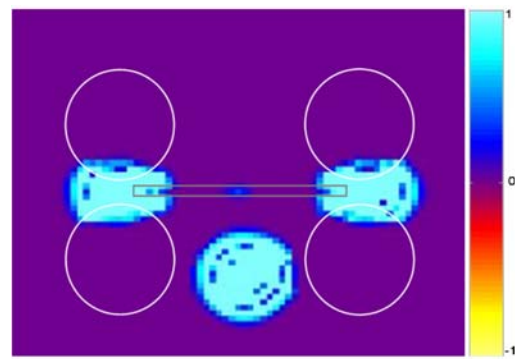

(a)

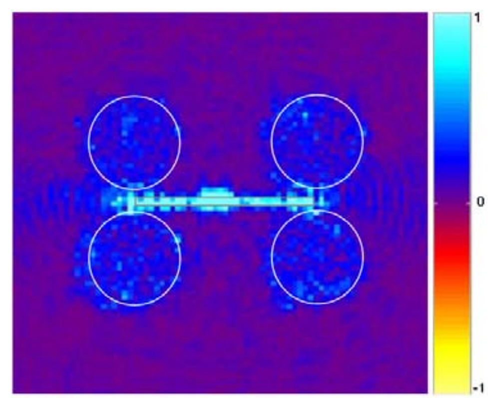

(b)

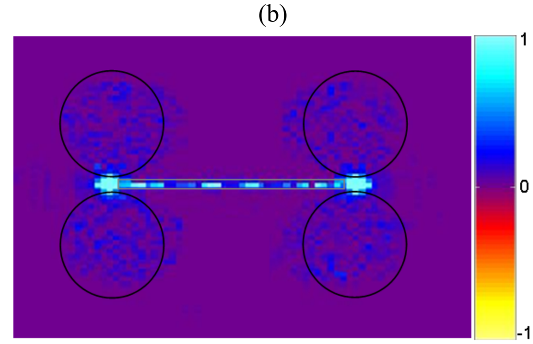

(c)

Fig. 4: Field pattern in the *xy* plan for structure 3 (a), (a) Field localization at transient state between nanospheres at both ends of NW and a third source is below and close to the center of NW (b) Electric field pattern at steady state, (c) Magnetic field pattern at steady state.

It shows that the dominant mode with quantum effects is at 21.96 eV, while without quantum effects is at 22.65 eV, and the difference of 0.69 eV is observed. These results are observed at a point on NW, when the distance between nanospheres is 5 nm. This plot shows that the field values near to 0 eV with quantum effects is smoother, as compared to the other curve (without quantum effect) that shows some abnormality, and the reason is absence of quantum effects. The proposed approach may have potential applications in the fields of active nano-plasmonics, optoelectronics, integration of nano-plasmonis and nano-electronics, and nano-sensors.

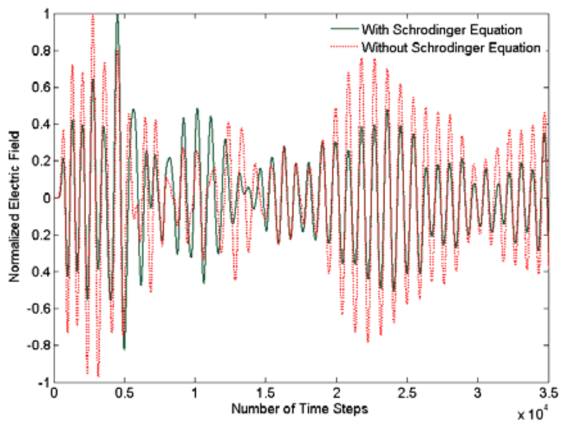

(a)

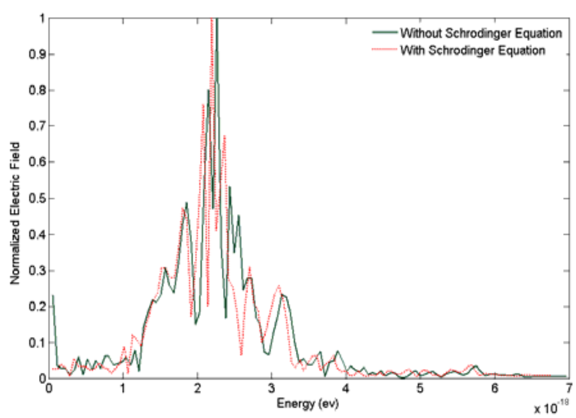

(b)

Fig. 5: Field plot for structure 3(a), (a) Electric field with respect to number of time steps with and without Schrödinger equation, b) Electric field with respect to energy (eV) with and without Schrödinger equation.

4. Conclusion

An approach that couples time dependent Schrödinger and LD dispersive model incorporated Maxwell equations is developed and implemented for plasmonics nanodevices and the FDTD method is applied for analysis. The approach is applied to structures that involve both dispersive and quantum effects. Results are compared with and without quantum effects and clear difference is observed among them. However, both approaches did not show any difference in numerical results for bulk materials. The proposed approach paves the way for modeling and simulation of nanodevices in the wide spectrum of electromagnetics, and where quantum effects are needed.

REFERENCES

1. S. A. Maier, *Plasmonics: Fundamentals and Applications*, 2007, Springer, New York, USA.
2. M. L. Brongersma, P. G. Kik, *surface Plasmon nanophotonics*, 2007, Springer, The Netherlands.
3. V. M. Shalaev and S. Kawata, *Nanophotonics with Surface Plasmons*, 2007, Elsevier.
4. R. Zia, and M. L. Brongersma, "Surface plasmon polariton analogue to Young's double-slit experiment," *Nature Nanotech*. 2, 426- 429, 2007.
5. E. H. Khoo, I. Ahmed and E. P. Li, "Investigation of the light energy extraction efficiency using surface modes in electrically pumped semiconductor microcavity", *Proc. SPIE* 7764, 77640B, 2010.
6. I. Ahmed, E. H. Khoo, O. Kurniawan, and E. P. Li, "Modeling and simulation of active plasmonics with the FDTD method by using solid state and Lorentz–Drude dispersive model", *J. of opt. Society B*, Vol. 28, No. 3, 352–359,. 2011.
7. O. Kurniawan, I. Ahmed and E. P. Li, "Development of a palsmonics source based on nano-antenna concept for nano-photonics applications" *IEEE Photonics Journal*, Vol. 3, pp. 344 – 352, 2011.
8. K. F. MacDonald, Z. L. Samson, M. I. Stockman and N. I. Zheludev, "Ultrafast active plasmonics" *Nature Photonics*, **3,** 55-58, 2009.
9. J. A. Dionne, K. Diest, L. A. Sweatlock, and H. A. Atwater, "Plas-MOStor: A metal-oxide-Si field effect plasmonic modulator," *Nano Letters*, **9**, 897-902, 2009.
10. A. V. Krasavin and A. V. Zayats, "Three-dimensional numerical modeling of photonics integration with dielectric loaded SPP waveguides", *Physics Review B*, **78**, 045425-8, 2008.
11. G. Naik and A. Boltasseva, "Plasmonics and metamaterials: looking beyond gold and silver", *SPIE, Newsroom*, January, 2012.
12. L. Pierantoni, D. Mencarelli and T. Rozzi, "A new 3-D transmission line matrix scheme for the combined Schrödinger Maxwell problem in the electronic electromagnetic characterization of nanodevices", *IEEE Trans. Micro. Theo. and Tech.*, Vol. 56, No. 3, 654-662, 2008.
13. I. Ahmed, Li, E. P. and R. Mittra "A Hybrid Approach for solving coupled Maxwell and Schrödinger equations arising in the simulation of nanodevices" *IEEE Anten. Wirel. Propag. Letts*, Vol. 9, 914-917, 2010.
14. D.G. Swanson, and W. J. R. Hofer, *Microwave circuit modeling using electromagnetic field simulation,* Artech House Inc. Norwood , MA, 2003.

15. A. Taflove and S. C. Hagness, *Computational Electrodynamics: The Finite-Difference Time-Domain Method,* 3rd Ed., Artech House, Boston, 2005.
16. I. Ahmed, E. K. Chua, E. P. Li, and Z. Chen, "Development of the three dimensional unconditionally stable LOD-FDTD method," *IEEE Trans. Antennas Propag.*, vol. 56, no. 11, pp. 3596–3600, Nov. 2008.
17. D. Rakic, A. B. Djurisic, J. M. Elazar and M. L. Majewski "Optical properties of Metallic films for vertical-cavity optoelectronic devices" *Apl. Optics*. **37,** 5271-5283, 1998.
18. D. M. Sullivan, *Electromagnetic simulation using the FDTD method*, 2000, Wiley-IEEE Press